Tunable Nanowire Patterning Using Standing Surface Acoustic Waves

Yuchao Chen,[†] Xiaoyun Ding,[†] Sz-Chin Steven Lin,[†] Shikuan Yang,[†] Po-Hsun Huang,[†] Nitesh Nama,[†] Yanhui Zhao,[†] Ahmad Ahsan Nawaz,[†] Feng Guo,[†] Wei Wang,[‡] Yeyi Gu,[§] Thomas E. Mallouk,[‡] and Tony Jun Huang[†,*]

[†]Department of Engineering Science and Mechanics, The Pennsylvania State University, University Park, Pennsylvania 16802, United States, [‡]Department of Chemistry, The Pennsylvania State University, University Park, Pennsylvania 16802, United States, and [§]Department of Food Science, The Pennsylvania State University, University Park, Pennsylvania 16802, United States

ABSTRACT Patterning of nanowires in a controllable, tunable manner is important for the fabrication of functional nanodevices. Here we present a simple approach for tunable nanowire patterning using standing surface acoustic waves (SSAW). This technique allows for the construction of large-scale nanowire arrays with well-controlled patterning geometry and spacing within 5 s. In this approach, SSAWs were generated by interdigital transducers, which induced a periodic alternating current (ac) electric field on the piezoelectric substrate and consequently patterned metallic nanowires in suspension. The patterns could be deposited onto the substrate after the liquid evaporated. By controlling the distribution of the SSAW field, metallic nanowires were assembled into different patterns including parallel and perpendicular arrays. The spacing of the nanowire arrays could be tuned by controlling the frequency of the surface acoustic waves. Additionally, we observed 3D spark-shaped nanowire patterns in the SSAW field. The SSAW-based nanowire-patterning technique presented here possesses several advantages over alternative patterning approaches, including high versatility, tunability, and efficiency, making it promising for device applications.

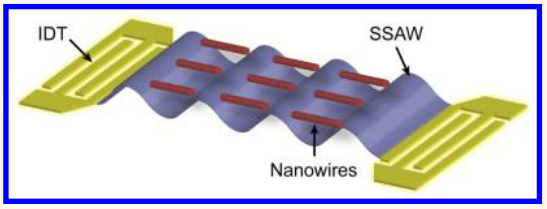

KEYWORDS: surface patterning · nanowire · standing surface acoustic waves (SSAW) · virtual electrodes

Nanowires are critical components in diverse applications, including chemical/biomolecular sensing,[1−6] nanoscale electronic circuits,[7−10] and optoelectronics.[11−13] Over the past two decades, researchers have made significant progress in the synthesis of different kinds of nanowires.[14−16] However, postsynthesis manipulation (alignment, patterning, assembly, and interconnection) of the nanowires is usually required for device applications.[17] To address this need, a variety of techniques have been developed for manipulating nanowires, including Langmuir−Blodgett assembly and transfer,[18−20] dielectrophoretic assembly,[21−24] magnetic alignment,[25] microfluidic approaches,[26−28] microcontact printing,[29−31] and lithographic strategies.[32,33] Each of these methods has its advantages and limitations. For example, in the dielectrophoretic approach, the positioning of individual nanowires is determined by the arrangement of alignment electrodes and/or wells that are first patterned lithographically.[34] Thus, the development of more flexible and tunable dielectrophoretic methods would be valuable in several applications. For example, highly aligned nanowire bundles can dramatically increase the sensitivity of surface-enhanced Raman spectroscopy (SERS) for chemical and biomolecular sensing.[1,35] However, current assembly methods provide inadequate control over the positioning of closely spaced nanowires, which strongly modulates the SERS signal intensity.[36] Therefore, a new approach that can generate controllable, tunable patterns is desirable. Herein, we demonstrate a standing surface acoustic wave (SSAW)-based nanopatterning technique, which enables the generation of tunable nanowire patterns either in suspension or on the surface of the substrate.

Previously, we have used SSAW-based methods to manipulate (*i.e.*, pattern, focus, and separate) electronically insulating microspheres or cells.[37−44] In these earlier studies, acoustic radiation forces caused by pressure fluctuations in the liquid played a major role in the manipulation of microscale objects,

* Address correspondence to junhuang@psu.edu.

Received for review January 1, 2013 and accepted March 29, 2013.

Published online 10.1021/nn4000034

driving them to pressure nodes or antinodes. In contrast, we take advantage here of the SSAW-induced piezoelectric field[45,46] to align and pattern metallic (*i.e.*, silver) nanowires by dielectrophoresis. SSAWs induce a nonuniform charge distribution and create virtual electrodes[47] on the piezoelectric substrate. By controlling the distribution of the SSAW field, virtual electrode arrays are easily repatternable, allowing for the manipulation of nanowires in real time. This flexibility is unattainable for most conventional approaches,[18−34,48] which ordinarily generate static patterns.

In this article, we demonstrate versatile, tunable patterning of nanowires into parallel and perpendicular arrays, as illustrated in Figure 1. In a SSAW-induced ac electric field, disordered nanowires (Figure 1A) suspended in liquid are aligned and assembled along the electric field lines (Figure 1D). With the application of one-dimensional (1D) SSAW, the nanowires are assembled into parallel rows with the same orientation (Figure 1B). In two-dimensional (2D) SSAW fields, the nanowires form a 2D lattice (Figure 1C) with 3D spark patterns at the nodes of the network (Figure 1E). Because the pitch of both the 1D and 2D structures is sensitive to the frequency of the SSAW field, this technique allows for the patterning of nanowires with tunable spacing and density.

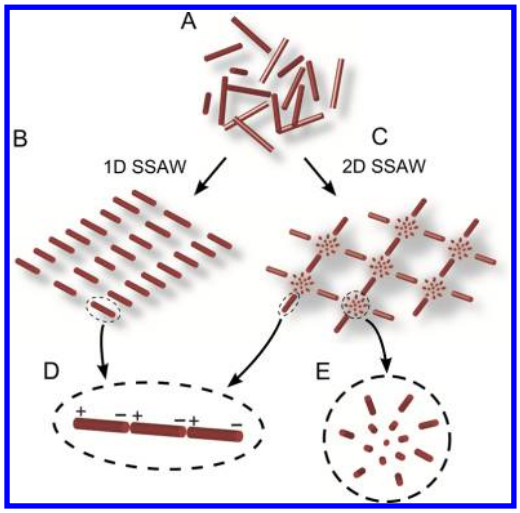

Figure 1. Schematic of the SSAW-assisted nanowire patterning technique. (A) Nanowires are randomly dispersed in solution. (B) 1D and (C) 2D SSAW fields induce the formation of nanowire arrays. (D) In the patterning process, nanowires are assembled into bundles due to the electric fields. (E) In the 2D patterning, 3D spark structures were observed at the nodes of the network.

RESULTS AND DISCUSSION

Mechanism of 1D Nanowire Patterning. Parallel nanowire arrays were assembled using a 1D SSAW field as illustrated in Figure 2A (see Supporting Information, Figure S1 A and B for device details). Two parallel interdigital transducers (IDTs) were deposited on a piezoelectric substrate (Y-128° $LiNbO_3$) to generate traveling surface acoustic waves (SAWs) along the *x* axis and form a 1D SSAW field. To study the mechanism of nanowire patterning, we used two parallel IDTs that had 20 pairs of electrodes with electrode widths and spacing gaps of 75 μm. Both IDTs could generate identical SAWs with a wavelength of 300 μm at a resonance frequency of 12.6 MHz. The input power was optimized between 50 and 80 mW considering the intensity of dielectric forces and the fluidic streaming effect (Supporting Information, Figure S2).[49] We used silver nanowires as a model in this study because of their wide applications in photonics, electronics, and biosensors.[50−58] Ag nanowire suspensions were injected into a 10 $\times$ 10 mm^2 open microchamber with a depth of 50 μm between the $LiNbO_3$ substrate and a glass slide. The patterning process was observed in dark field using an optical microscope.

Figure 2B presents a cross-sectional view of the piezoelectric substrate along the *x* axis to illustrate the mechanism of nanowire patterning in a 1D SSAW field. The standing mechanical vibrations along the *z* axis induce a nonuniform charge distribution on the $LiNbO_3$ substrate. The periodic displacement nodes (minimum displacement) correspond to SSAW pressure antinodes. When placed in the SSAW field, polystyrene microspheres are driven to the displacement antinodes (pressure nodes) with a consistent spacing of half the wavelength, as shown in previous studies.[39] The periodic distribution of electric charges generates an ac electric field with electric field lines from positive charges to negative charges. The electric field was simulated using COMSOL Multiphysics 3.5a software (Figure 2C). Polarized by the electric field, nanowires are aligned to the field lines along the *x* axis (SAW propagation direction) due to resultant torques. Then, dielectrophoretic forces transport the nanowires to the displacement nodes, where the nanowires experience counter-balancing forces from both positive and negative electric charges. To test this hypothesis, we placed both silver nanowires and polystyrene microspheres in SSAW fields to observe their relative locations, as shown in Figure 2D. Unlike microspheres, which were trapped at the pressure nodes, nanowires were patterned into parallel arrays along the displacement nodes (pressure antinodes). This observation was consistent with our hypothesis that nanowires are patterned by dielectrophoretic forces rather than by acoustic radiation forces.

To further study the forces exerted on nanowires, we carried out another control experiment by inserting a layer of coupling liquid (water) and a Au layer between the $LiNbO_3$ substrate and the nanowire suspension (see Supporting Information, Figure S1C for device details). The Au layer was designed to shield the nanowires from the electric field. As a result, the dielectrophoretic forces were significantly screened, whereas the acoustic wave could still transmit into the nanowire suspension through the coupling liquid. Dominated by acoustic radiation

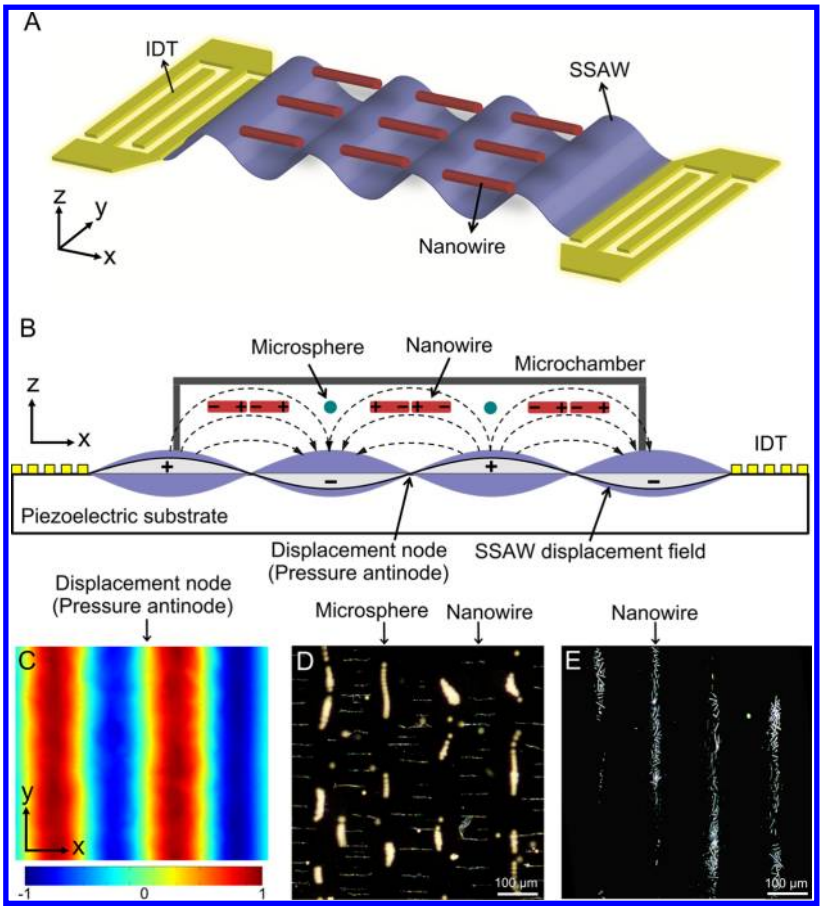

Figure 2. (A) Schematic of 1D nanowire patterning. Two parallel IDTs generate SSAW to align and pattern nanowires in the suspension. (B) Cross-section view of IDT-deposited piezoelectric substrate along the *x* axis. The mechanical vibration of the substrate is induced by SSAW, and the electric field is generated by nonuniform charge distribution. Nanowires and microspheres are patterned in the microchamber due to dielectrophoretic forces and acoustic radiation forces, respectively. (C) Simulation result shows the periodic electric field distribution induced by the 1D SSAW. The values of the color bar are normalized. (D) Patterning of nanowires and microspheres in 1D SSAW field to show their relative positions. (E) By screening the nanowire suspension from the electric field, a control experiment demonstrates that, in the absence of dielectrophoretic forces, nanowire bundles are trapped at pressure nodes (displacement antinodes) by acoustic radiation forces and do not align.

forces, the nanowire bundles had similar behaviors to microspheres, which were patterned at pressure nodes without alignment by the electric field (Figure 2E). This control experiment indicates that although metallic nanowires experience both dielectrophoretic and acoustic radiation forces inside a SSAW field, the dielectrophoretic forces play a dominant role in their patterning. In our calculation (see Supporting Information), the acoustic radiation force and dielectric force acting on a nanowire bundle (length ~50 μm, radius ~250 nm) were estimated to be 0.24 pN and 700 pN, respectively. The acoustic radiation force is smaller than the dielectric force by approximately 3 orders of magnitude.

Patterning Nanowires in Suspension. We demonstrate that our method can manipulate and pattern suspended nanowires in a real-time fashion. As the propagation direction of SAWs changes, the alignment direction of the nanowires can be switched simultaneously, allowing for dynamic patterning. As soon as the input power is turned off, the nanowire arrays are disturbed by the fluidic flow, but they can be repatterned into various geometries by applying different SSAW fields. It was also possible to switch between patterns without turning off the power during the process. The dynamic patterning concept is illustrated in Figure 3. After turning off the radio frequency (RF) signal, patterned nanowire bundles were randomly distributed in the suspension (Figure 3A). When polarized again by the SSAW-induced 1D electric field, small nanowire bundles simultaneously connected end-to-end to form a longer chain of wires, which took less than 1 s (Figure 3B). Due to the dielectrophoretic forces along the *x* and *y* directions,[24] these bundles tended to move close to each other while reorienting along the SAW propagation direction (Figure 3C). During this process, some bundles would merge together as shown in Figure 3D and E. The red arrows in Figure 3D and E indicate a typical combination process of two nanowire bundles located in close proximity. Finally, all the nanowire bundles were aligned and patterned into one row anchored in the SSAW displacement node (pressure antinode) with almost the same spacing along the *y* direction (Figure 3F). The whole process took about

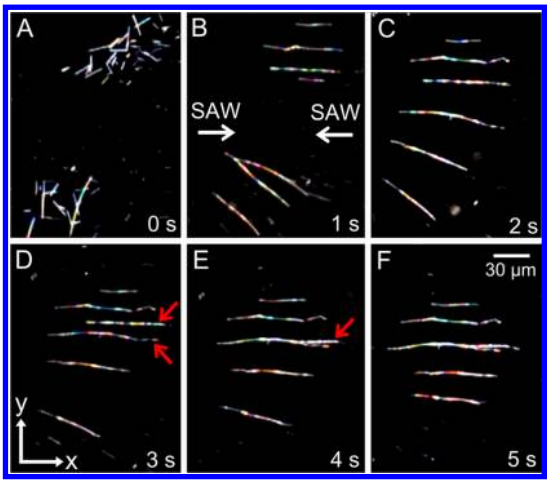

Figure 3. Dynamic process of nanowire patterning in a 1D SSAW field. The images were taken in 1 s interval for 5 s. The white arrows in (B) show the propagation direction of SAWs. The red arrows in (D) and (E) indicate a typical combination process of two adjacent nanowire bundles.

5 s, which was comparable to the conventional dielectrophoretic approach.[21] A stable pattern of nanowires was achieved when the electrostatic repulsion forces from neighboring nanowire bundles, and dielectrophoretic forces along the *y* direction were properly balanced, resulting in a very regular spacing of nanowire bundles (Supporting Information, Figure S3).[34]

Patterning Nanowires on Substrates. Patterning nanowires onto the surface of a substrate is important in many applications, particularly in the fabrication of optical and electrical devices. In the SAW-assisted patterning technique, we have shown that Ag nanowires can be patterned in suspension (Figure 3). We also found that the nanowire patterns could settle down from the suspension onto the piezoelectric substrate without destroying the patterns (Figure 4). Before the SSAW field was applied, the nanowires were dispersed in the microchamber (Figure 4A). A few nanowire clusters were observed as bright dots by a

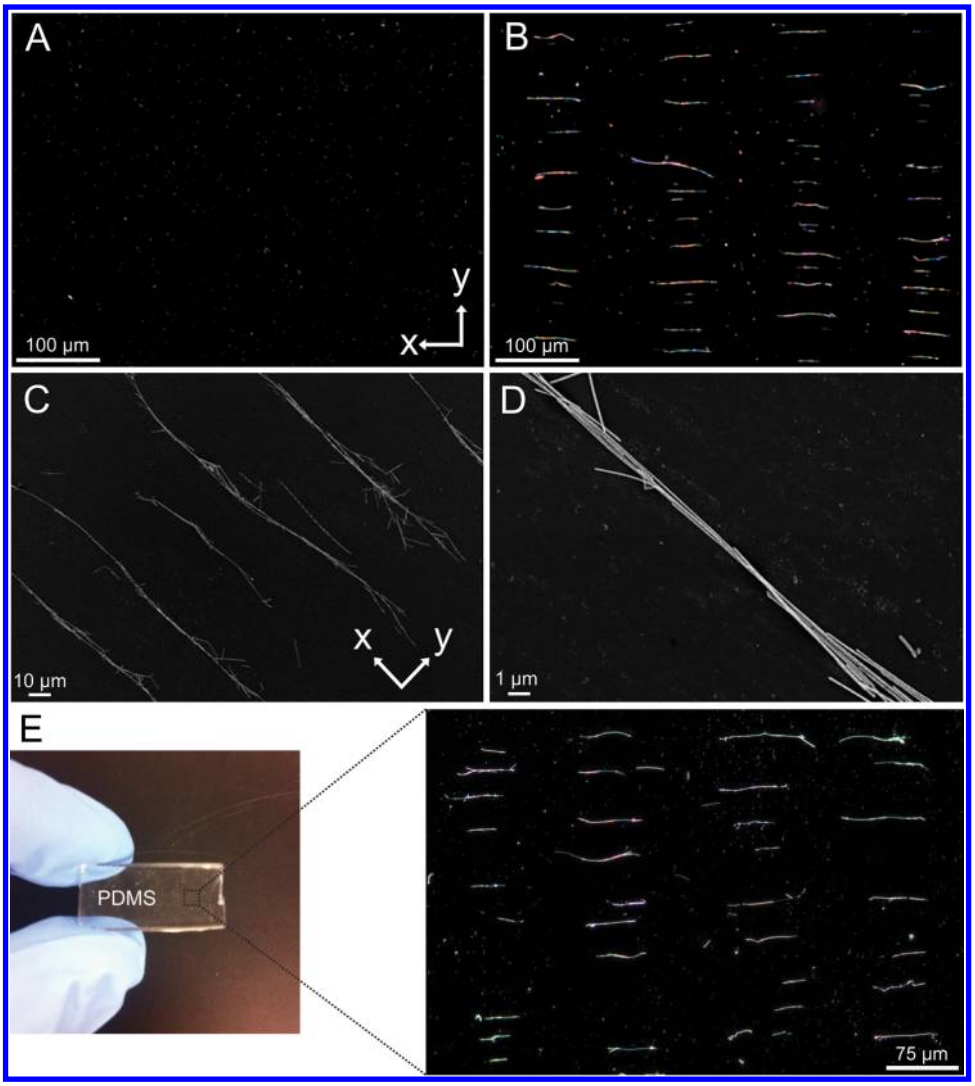

Figure 4. Surface patterning of nanowires. (A) Before applying the SSAW, nanowires uniformly dispersed in the suspension. (B) Nanowires aligned and patterned in the suspension when applying a 1D SSAW field. SEM images of (C) aligned nanowire bundles on the substrate and (D) a typical nanowire bundle within the surface patterns. (E) Dry transfer of nanowire patterns with polydimethylsiloxane (PDMS) stamp.

dark-field microscope. When a 1D SSAW field was applied, the nanowires were polarized and subsequently assembled into bundles with the long axis along the propagation direction of the SAWs (*x* direction), as shown in Figure 4B. Ultimately, aligned nanowires were patterned into parallel rows located at the SSAW displacement nodes (pressure antinodes), perpendicular to the SAW propagation direction (in the *x* direction). The average length of the nanowire bundles and their average spacing along the *y* direction were dependent on the concentration and, therefore, could be controlled by adjusting the nanowire concentration in the suspension (Supporting Information, Figure S4). The spacing of nanowire arrays along the *x* direction (distance between the centers of two adjacent rows) was around 150 μm, which was equivalent to the half-wavelength of the SSAWs. After the nanowires were patterned in the suspension, the liquid medium in the open chamber gradually evaporated within 2−3 min. The SSAWs were retained during the evaporation process to prevent the patterns from being destroyed by convection or capillary forces. Consequently, the nanowires patterned in the suspension were deposited onto the substrate. The integrity of the surface patterns is comparable to those in the freestanding suspension. A scanning electron microscope (SEM) image of nanowire surface patterns on a $LiNbO_3$ substrate is shown in Figure 4C. Most nanowire bundles were well aligned in the same direction after the liquid evaporated, with only a small number of nanowires changing their orientations. Figure 4D shows the structure of a typical nanowire bundle, in which the silver nanowires are assembled tightly into a bundle. After the nanowire patterns were deposited onto the $LiNbO_3$ substrate, they could be successfully transferred onto polydimethylsiloxane (PDMS) stamps with high fidelity (Figure 4E). The stamp was lightly attached onto the substrate to make a conformal contact. The nanowire patterns were then picked up with the PDMS stamp by peeling off the stamp with a high speed. It should be possible to redeposit the nanowires on these PDMS stamps to rigid or flexible substrates using microcontact printing techniques that are already well developed.[59−62]

Tunability of Nanowire Patterning. As demonstrated above, an SSAW-induced piezoelectric field can be used to prepare highly ordered nanowire bundles, which usually show distinct optical properties. Here, we further explored the ability of this SSAW-assisted patterning technique in tuning the structure of nanowire patterns (particularly, the spacing of nanowire bundles). The method allowed control of the spacing along the *x* direction by simply tuning the frequency of SSAWs. In the 1D SSAW field, nanowire bundles are patterned along the nodal positions with the spacing equal to the half-wavelength; therefore an SSAW with tunable frequency should be able to control the spacing of nanowires in real time. To illustrate this idea, two parallel chirped IDTs,[41] which generated two traveling SAWs and formed a 1D SSAW field, were used to control the spacing of nanowires along the *x* direction. The chirped IDTs had a gradient width of the electrode (25−50 μm), which could generate SAWs with different wavelengths (100−200 μm) at a resonance frequency between 18.5 and 37 MHz. A nanowire suspension with a concentration of 10 μg/mL was used for patterning, and the results are shown in Figure 5. As the frequency of SSAW gradually increased, nanowire bundles in different rows were moved closer to each other along the *x* direction due to the decrease in the wavelength of the SSAW. The average spacing measured at different frequencies produced values similar to each frequency's corresponding half-wavelength. For example, at the frequency of 19 MHz and a half-wavelength of 100 μm, the average spacing was 97.6 μm. When the frequency increased to 37 MHz, resulting in a corresponding half-wavelength of 50 μm, the average spacing decreased to 48.4 μm. The insets of Figure 5 show that the density of nanowire bundles in the pattern increases with the frequency of the SSAW. By tuning the frequency, the shift of the nodal positions induced a rearrangement of the nanowire patterns.

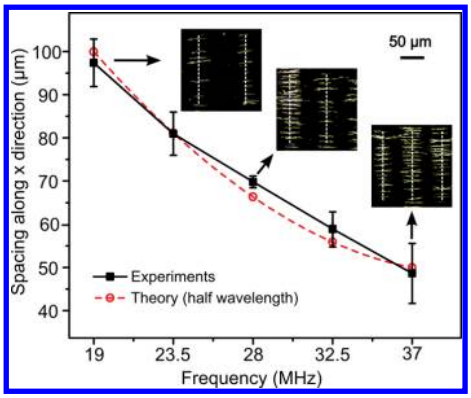

Figure 5. Spacing of nanowires along the *x* direction (horizontal axis in the inset images) as a function of SSAW frequency. Black squares represent the spacing of nanowires patterned by chirped IDTs at five frequencies from 19 to 37 MHz. Red open circles represent calculated values of nanowire spacing, which equals the acoustic half-wavelength. Insets show representative patterns of nanowires at frequencies of 19, 28, and 37 MHz. White dashed lines in the inset images indicate the centers of each row.

The ability to control the structure of nanowire patterns renders the SSAW-based method a versatile tool for nanowire alignment and surface patterning. The 1D parallel nanowire array is one of the most commonly used nanowire patterns with applications that include molecular sensors,[3] nanowire transistors,[63] and nanowire batteries.[64] Compared to the conventional dielectrophoretic approach, this technique does not require prefabricated electrodes and is more versatile in that the spacing and orientation can be tuned *in situ*.

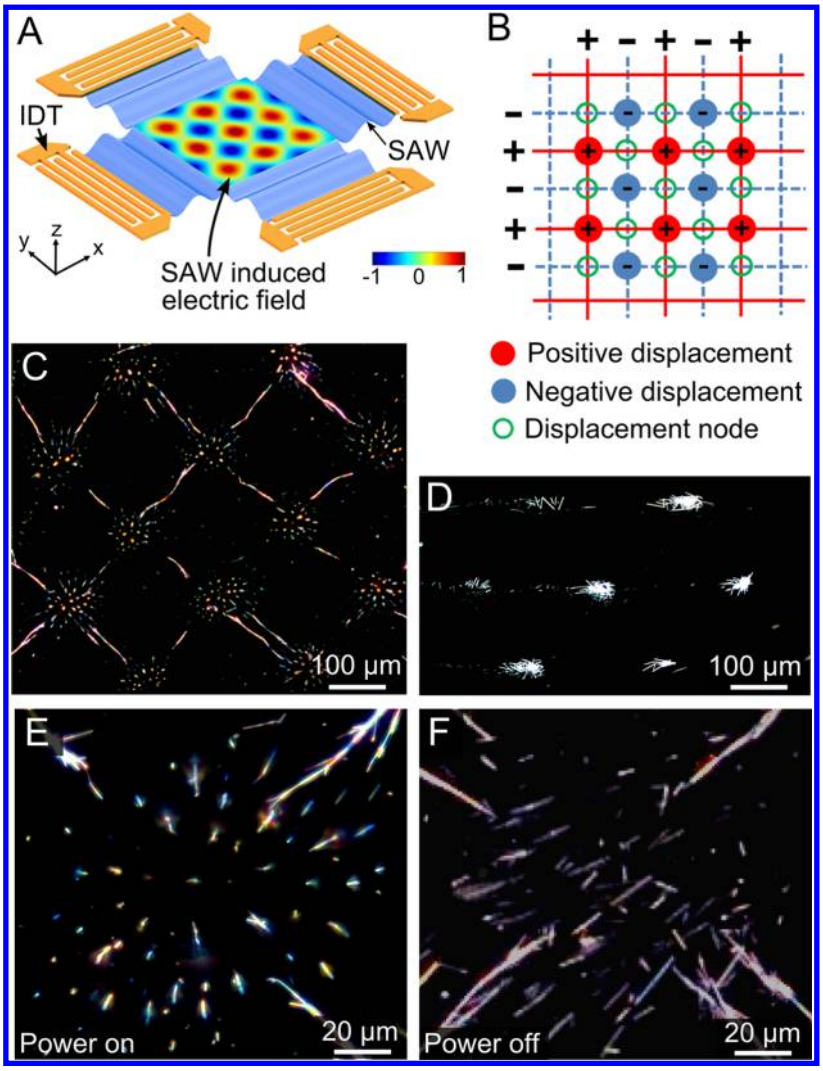

Figure 6. (A) Simulation of the electric field distribution in a 2D SSAW field. The values of the color bar are normalized. (B) Mechanism of 2D displacement field distribution. Red lines represent maximum positive displacements that carry positive charges. Blue lines represent maximum negative displacements that carry negative charges. (C) Image of 2D nanowire patterning. 3D nanowire spark patterns are positioned at the displacement antinodes (pressure nodes). (D) Control experiment in which the nanowire suspension is screened from the electric field. Nanowires are trapped at the pressure nodes (displacement antinodes) by acoustic radiation forces. (E) Zoom-in of 3D nanowire spark pattern in (C). (F) After turning off the power, nanowires in the spark pattern settle in the suspension.

2D Patterning of Nanowires. 2D SSAW fields could also be generated, resulting in nanowires patterned into perpendicular arrays. Figure 6A shows a simulation of a 2D electric field generated by two orthogonal pairs of IDTs. An array of virtual dot electrodes was created on the piezoelectric substrate due to the interaction between the two orthogonal SSAWs, a result that was quite different from the 1D simulation results (see Figure 2C). Figure 6B illustrates the mechanism of the formation of a 2D electric field. When 2D SSAW was generated, the interaction of positive displacement antinodes (red lines) formed antinode points with positive charges (red filled circles), and the interaction of negative antinodes (blue lines) formed antinode points with negative charges (blue filled circles). Nodes in the 2D displacement field (green open circles), which had no displacement, were located at the positions that were equidistant from the positive and negative antinodes. The electric field lines between the positive and negative antinodes aligned the nanowires in perpendicular directions, as shown in Figure 6C. 2D networks were formed with angles of 90° between the nanowire bundles. Nanowires patterned into 3D spark structures were observed at the displacement antinodes due to the high intensity of the electric field. A control experiment similar to 1D patterning was carried out by screening the electric field (Figure 6D). Nanowire bundles were trapped at the SSAW pressure nodes, which showed a different pattern from the one generated by the electric field. After careful examination of the 3D spark structure in Figure 6E, it was found that the nanowire bundles were aligned along the electric field lines with one end pointing toward the displacement antinodes. When the power was off, the

nanowire bundles stopped spinning and settled in the suspension, as shown in Figure 6F. In addition, the nanowire bundles in the spark structure appeared to become longer after turning off the power, indicating that they had been aligned along different tilt directions in a 3D configuration in the electric field.

CONCLUSIONS

Nanowires can be controllably patterned into different geometries in a rapid, simple process by using electric fields generated by SSAW. The spacing of nanowire bundles can be adjusted by tuning the frequency of the SSAW. With 1D SSAW patterns, the direction of nanowire alignment can be reoriented in real time, and 1D and 2D patterns are interconvertible by switching the distribution of the SSAW field. The SSAW-based method therefore offers a new dimension of versatility and tunability to dielectrophoretic patterning of metal nanowires. As a contactless and template-free patterning technique, SSAW patterning of nanowires may be useful in diverse applications that include electronics, biotechnology, and microfluidics.

MATERIALS AND METHODS

Device Fabrication and Experimental Setup. In this study, we used Y+128° X-propagation lithium niobate ($LiNbO_3$) as piezoelectric substrates. To deposit IDTs on the substrate, the $LiNbO_3$ wafer was spin-coated with a layer of photoresist (SPR3012, MicroChem, Newton, MA, USA). The IDT design on the mask was transferred by UV exposure and then developed in a photoresist developer (MF CD-26, Microposit). After depositing a metal double layer (Cr/Au, 50 Å/500 Å) with an e-beam evaporator (Semicore Corp), IDTs were formed by a lift-off process.

Two spacers with a height of 50 μm were created by attaching polyimide Kapton tapes on the substrate. After covering with a glass slide (10 $\times$ 10 mm^2) on the top, an open microchamber between the glass slide and the substrate was formed to contain the nanowire suspension. In the control experiments, two open microchambers were created to form a coupling liquid (water) layer at the bottom and a suspension layer at the top (Supporting Information, Figure S1).

The device was immobilized on the stage of a microscope (Nikon, Eclipse Ti, LV100DA-U). A camera (Nikon, DS-Fi1) was connected to the microscope to capture the dynamics of nanowire patterning in dark field. An RF signal generator (Agilent Tech, E4422B) connected to the IDTs provided coherent ac signals at a frequency of 12.6 MHz with input powers from 10 to 250 mW to generate SSAWs on the piezoelectric substrate (Supporting Information, Figure S2). When chirped IDTs were used, the frequency of the acoustic waves could be tuned by controlling the input frequency of the ac signals.

Preparation of Silver Nanowire Suspension. Silver nanowires were purchased from Blue Nano (NC, USA). The nanowires had average diameters and lengths of 60 nm and 40 μm, respectively. The nanowires were dispersed in ethanol at an original concentration of 7 mg/mL, and the suspensions were then diluted by adding deionized water to a final concentration of 5−45 μg/mL (Supporting Information, Figure S5). The diluted nanowire suspensions were then sonicated for 15 min to disperse aggregates and resuspend the nanowires.

SEM Image of Nanowires. SEM images were taken on dried nanowires deposited on the surface of the piezoelectric substrate. After the nanowires were patterned by the SSAW fields, we kept the acoustic power on until the liquid evaporated to deposit the nanowire patterns on the surface.

Conflict of Interest: The authors declare no competing financial interest.

Acknowledgment. We gratefully acknowledge financial support from National Institutes of Health (Director's New Innovator Award, 1DP2OD007209-01), the National Science Foundation, and the Penn State Center for Nanoscale Science (MRSEC) under grant DMR-0820404. Components of this work were conducted at the Penn State node of the NSF-funded National Nanotechnology Infrastructure Network. We thank Joey Rufo for his helpful discussion.

Supporting Information Available: (1) Device configuration; (2) patterning time; (3) force analysis; (4) dependence of nanowire patterns on sample concentration; (5) estimation of acoustic radiation force and dielectric force. This material is available free of charge *via* the Internet at http://pubs.acs.org.

REFERENCES AND NOTES

1. Tao, A.; Kim, F.; Hess, C.; Goldberger, J.; He, R.; Sun, Y.; Xia, Y.; Yang, P. Langmuir-Blodgett Silver Nanowire Monolayers for Molecular Sensing Using Surface-Enhanced Raman Spectroscopy. *Nano Lett.* **2003**, *3*, 1229–1233.
2. Bangar, M. A.; Shirale, D. J.; Chen, W.; Myung, N. V.; Mulchandani, A. Single Conducting Polymer Nanowire Chemiresistive Label-Free Immunosensor for Cancer Biomarker. *Anal. Chem.* **2009**, *81*, 2168–2175.
3. Lee, S. J.; Morrill, A. R.; Moskovits, M. Hot Spots in Silver Nanowire Bundles for Surface-Enhanced Raman Spectroscopy. *J. Am. Chem. Soc.* **2006**, *128*, 2200–2201.
4. Mcalpine, M. C.; Ahmad, H.; Wang, D.; Heath, J. R. Highly Ordered Nanowire Arrays on Plastic Substrates for Ultrasensitive Flexible Chemical Sensors. *Nat. Mater.* **2007**, *6*, 379–384.
5. Ramanathan, K.; Bangar, M. A.; Yun, M.; Chen, W.; Myung, N. V.; Mulchandani, A. Bioaffinity Sensing Using Biologically Functionalized Conducting-Polymer Nanowire. *J. Am. Chem. Soc.* **2005**, *127*, 496–497.
6. Kim, J. H.; Heller, D. A.; Jin, H.; Barone, P. W.; Song, C.; Zhang, J.; Trudel, L. J.; Wogan, G. N.; Tannenbaum, S. R.; Srano, M. S. The Rational Design of Nitric Oxide Selectivity in Single-walled Carbon Nanotube Near-Infrared Fluorescence Sensors for Biological Detection. *Nat. Chem.* **2009**, *1*, 473–481.
7. Dayeh, S. A.; Aplin, D. P. R.; Zhou, X.; Yu, P. K. L.; Yu, E. T.; Wang, D. High Electron Mobility InAs Nanowire Field-Effect Transistors. *Small* **2007**, *3*, 326–332.
8. Dehon, A. Array-Based Architecture for FET-Based, Nanoscale Electronics. *IEEE Trans. Nanotech.* **2003**, *2*, 23–32.
9. Beckman, R.; Johnston-Halperin, E.; Luo, Y.; Green, J. E.; Heath, J. R. Bridging Dimensions: Demultiplexing Ultrahigh-Density Nanowire Circuits. *Science* **2005**, *310*, 465–468.
10. Yan, H.; Choe, H. S.; Nam, S. W.; Hu, Y. J.; Das, S.; Klemic, J. F.; Ellenbogen, J. C.; Lieber, C. M. Programmable Nanowire Circuits for Nanoprocessors. *Nature* **2011**, *470*, 240–244.
11. Heng, L.; Zhai, J.; Qin, A.; Zhang, Y.; Wen, Y.; Tang, B.; Jiang, L. Fabrication of Hexaphenylsilole Nanowires and Their Morphology-Tunable Photoluminescence. *ChemPhysChem* **2007**, *8*, 1513–1518.
12. Tian, B. Z.; Zheng, X. L.; Kempa, T. J.; Fang, Y.; Yu, N. F.; Yu, G. H.; Huang, J. L.; Lieber, C. M. Coaxial Silicon Nanowires as Solar Cells and Nanoelectronic Power Sources. *Nature* **2007**, *449*, 885–889.
13. Yan, R.; Gargas, D.; Yang, P. Nanowire Photonics. *Nat. Photonics* **2009**, *3*, 569–576.
14. Freer, E. M; Krupp, L. E.; Hinsberg, W. D.; Rice, P. M.; Hedrick, J. L.; Cha, J. N.; Miller, R. D.; Kim, H.-C. Oriented Mesoporous Organosilicate Thin Films. *Nano Lett.* **2005**, *5*, 2014–2018.

15. Xia, Y.; Yang, P.; Sun, Y.; Wu, Y.; Mayers, B.; Gates, B.; Yin, Y.; Kim, F.; Yan, H. One-Dimensional Nanostructures: Synthesis, Characterization, and Application. *Adv. Mater.* **2003**, *15*, 353–389.
16. Yang, S.; Xu, J.; Wang, Z.; Zeng, H.; Lei, Y. Janus Particle Arrays with Multiple Structural Controlling Abilities Synthesized by Seed-directed Deposition. *J. Mater. Chem.* **2011**, *21*, 11930–11935.
17. Su, B.; Wu, Y.; Jiang, L. The Art of Aligning One-Dimensional (1D) Nanostructures. *Chem. Soc. Rev.* **2012**, *41*, 7832–7856.
18. Yang, P. D.; Kim, F. Langmuir-Blodgett Assembly of One-Dimensional Nanostructures. *ChemPhysChem* **2002**, *3*, 503–506.
19. Wang, D.; Chang, Y. L.; Liu, Z.; Dai, H. Oxidation Resistant Germanium Nanowires: Bulk Synthesis, Long Chain Alkanethiol Functionalization, and Langmuir-Blodgett Assembly. *J. Am. Chem. Soc.* **2005**, *127*, 11871–11875.
20. Mai, L.; Gu, Y.; Han, C.; Hu, B.; Chen, W.; Zhang, P.; Xu, L.; Guo, W.; Dai, Y. Orientated Langmuir-Blodgett Assembly of VO_2 Nanowires. *Nano Lett.* **2009**, *9*, 826–830.
21. Smith, P. A.; Nordquist, C. D.; Jackson, T. N.; Mayer, T. S.; Martin, B. R.; Mbindyo, J.; Mallouk, T. E. Electric-Field Assisted Assembly and Alignment of Metallic Nanowires. *Appl. Phys. Lett.* **2000**, *77*, 1399–1401.
22. Islam, M. A.; Xia, Y.; Steigerwald, M. L.; Yin, M.; Liu, Z.; O'Brien, S.; Levicky, R.; Herman, I. P. Addition, Suppression, and Inhibition in the Electrophoretic Deposition of Nanocrystal Mixture Films for CdSe Nanocrystals with γ-Fe_2O_3 and Au Nanocrystals. *Nano Lett.* **2003**, *3*, 1603–1606.
23. Raychaudhuri, S.; Dayeh, S. A.; Wang, D.; Yu, E. T. Precise Semiconductor Nanowire Placement through Dielectrophoresis. *Nano Lett.* **2009**, *9*, 2260–2266.
24. Freer, E. M.; Grachev, O.; Duan, X.; Martin, S.; Stumbo, D. P. High-Yield Self-limiting Single-Nanowire Assembly with Dielectrophoresis. *Nat. Nanotechnol.* **2010**, *5*, 525–530.
25. Tanase, M.; Bauer, L. A.; Hultgren, A.; Silevitch, D. M.; Sun, L.; Reich, D. H.; Searson, P. C.; Meyer, G. J. Magnetic Alignment of Fluorescent Nanowires. *Nano Lett.* **2001**, *1*, 155–158.
26. Huang, Y.; Duan, X.; Lieber, C. M. Directed Assembly of One-Dimensional Nanostructures into Functional Networks. *Science* **2001**, *291*, 630–633.
27. Park, J. U.; Meitl, M. A.; Hur, S. H.; Usrey, M. L.; Strano, M. S.; Kenis, P. J. A.; Rogers, J. A. *In Situ* Deposition and Patterning of Single-Walled Carbon Nanotubes by Laminar Flow and Controlled Flocculation in Microfluidic Channels. *Angew. Chem., Int. Ed.* **2006**, *45*, 595–599.
28. Messer, B.; Song, J. H.; Yang, P. Microchannel Networks for Nanowire Patterning. *J. Am. Chem. Soc.* **2000**, *122*, 10232–10233.
29. Fan, Z.; Ho, J. C.; Jacobson, Z. A.; Yerushalmi, R.; Alley, R. L.; Razavi, H.; Javey, A. Wafer-Scale Assembly of Highly Ordered Semiconductor Nanowire Arrays by Contact Printing. *Nano lett.* **2008**, *8*, 20–25.
30. Liu, H.; Takagi, D.; Chiashi, S.; Homma, Y. Transfer and Alignment of Random Single-Walled Carbon Nanotube Films by Contact Printing. *ACS Nano* **2010**, *4*, 933–938.
31. Takahashi, T.; Nichols, P.; Takei, K.; Ford, A. C.; Jamshidi, A.; Wu, M. C.; Ning, C. Z.; Javey, A. Contact Printing of Compositionally Graded CdS*x*Se1-*x* Nanowire Parallel Arrays for Tunable Photodetectors. *Nanotechnology* **2012**, *23*, 045201.
32. Colli, A.; Fasoli, A.; Pisana, S.; Fu, Y.; Beecher, P.; Milne, W. I.; Ferrari, A. C. Nanowire Lithography on Silicon. *Nano Lett.* **2008**, *8*, 1358–1362.
33. Islam, M. A.; Geiger, R. T.; Kim, J. A Novel Testbed Structure for Nanoshell Based Devices. *Nanotechnology* **2007**, *18*, 255203.
34. Smith, B. D.; Mayer, J. S.; Keating, C. D. Deterministic Assembly of Functional Nanostructures Using Nonuniform Electric Fields. *Annu. Rev. Phys. Chem.* **2012**, *63*, 241–263.
35. Choi, D.; Kang, T.; Cho, H.; Choia, Y.; Lee, L. P. Additional Amplifications of SERS *via* an Optofluidic CD-Based Platform. *Lab Chip* **2009**, *9*, 239–243.
36. Yang, S.; Cai, W.; Kong, L.; Lei, Y. Surface Nanometer-Scale Patterning in Realizing Large-Scale Ordered Arrays of Metallic Nanoshells with Well-Defined Structures and Controllable Properties. *Adv. Funct. Mater.* **2010**, *20*, 2527–2533.
37. Ding, X.; Lin, S.-C. S.; Lapsley, M. I.; Li, S.; Guo, X.; Chan, C. Y. K.; Chiang, I.-K.; McCoy, J. P.; Huang, T. J. Standing Surface Acoustic Wave (SSAW) Based Multichannel Cell Sorting. *Lab Chip* **2012**, *12*, 4228–4231.
38. Shi, J.; Mao, X.; Ahmed, D.; Colletti, A.; Huang, T. J. Focusing Microparticles in a Microfluidic Channel with Standing Surface Acoustic Waves (SSAW). *Lab Chip* **2008**, *8*, 221–223.
39. Shi, J.; Ahmed, D.; Mao, X.; Lin, S.-C. S.; Lawit, A.; Huang, T. J. Acoustic Tweezers: Patterning Cells and Microparticles Using Standing Surface Acoustic Waves (SSAW). *Lab Chip* **2009**, *9*, 2890–2895.
40. Shi, J.; Huang, H.; Stratton, Z.; Huang, Y.; Huang, T. J. Continuous Particle Separation in a Microfluidic Channel *via* Standing Surface Acoustic Waves (SSAW). *Lab Chip* **2009**, *9*, 3354–3359.
41. Ding, X.; Lin, S.-C. S.; Kiraly, B.; Yue, H.; Li, S.; Chiang, I.-K.; Shi, J.; Benkovicb, S. J.; Huang, T. J. On-Chip Manipulation of Single Microparticles, Cells, and Organisms Using Surface Acoustic Waves. *Proc. Natl. Acad. Sci. U.S.A.* **2012**, *109*, 11105–11109.
42. Lin, S.-C. S.; Mao, X.; Huang, T. J. Surface Acoustic Wave (SAW) Acoustophoresis: Now and Beyond. *Lab Chip* **2012**, *12*, 2766–2770.
43. Ding, X.; Shi, J.; Lin, S.-C. S.; Yazdi, S.; Kiraly, B.; Huang, T. J. Tunable Patterning of Microparticles and Cells using Standing Surface Acoustic Waves. *Lab Chip* **2012**, *12*, 2491–2497.
44. Shi, J.; Yazdi, S.; Lin, S.-C. S.; Ding, X.; Chiang, I.-K.; Sharp, K.; Huang, T. J. Three-Dimensional Continuous Particle Focusing in a Microfluidic Channel *via* Standing Surface Acoustic Waves (SSAW). *Lab Chip* **2011**, *11*, 2319–2324.
45. Strobl, C. J.; Schaflein, C.; Beierlein, U.; Ebbecke, J.; Wixforth, A. Carbon Nanotube Alignment by Surface Acoustic Waves. *Appl. Phys. Lett.* **2004**, *85*, 1427–1429.
46. Kong, X. H.; Deneke, C.; Schmidt, H.; Thurmer, D. J.; Ji, H. X.; Bauer, M.; Schmidt, O. G. Surface Acoustic Wave Mediated Dielectrophoretic Alignment of Rolled-up Microtubes in Microfluidic Systems. *Appl. Phys. Lett.* **2010**, *96*, 134105.
47. Jamshidi, A.; Pauzauskie, P. J.; Schuck, P. J.; Ohta, A. T.; Chiou, P.-Y.; Chou, J.; Yang, P.; Wu, M. C. Dynamic Manipulation and Separation of Individual Semiconducting and Metallic Nanowires. *Nat. Photonics* **2008**, *2*, 86–89.
48. Islam, M. A.; Xia, Y.; Telesca, D. A., Jr.; Steigerwald, M. L.; Herman, I. P. Controlled Electrophoretic Deposition of Smooth and Robust Films of CdSe Nanocrystals. *Chem. Mater.* **2004**, *16*, 49–54.
49. Friend, J.; Yeo, L. Y. Microscale Acoustofluidics: Microfluidics Driven *via* Acoustics and Ultrasonics. *Rev. Mod. Phys.* **2011**, *83*, 647–704.
50. Huang, T. J.; Liu, M.; Knight, L. D.; Grody, W. W.; Miller, J. F.; Ho, C.-M. An Electrochemical Detection Scheme for Identifications of Single-Nucleotide Polymorphism Using Hairpin-Forming Probes. *Nucleic Acids Res.* **2002**, *30*, e55.
51. Hsiao, V. K. S.; Waldeisen, J. R.; Zheng, Y.; Lloyd, P. F.; Bunning, T. J.; Huang, T. J. Aminopropyltriethoxysilane (APTES)-Functionalized Nanoporous Polymeric Gratings: Fabrication and Application in Biosensing. *J. Mater. Chem.* **2007**, *17*, 4896–4901.
52. Zheng, Y. B.; Desai, A. Y.; Wang, S. J.; Tan, L. K.; Gao, H.; Huan, A. C. H.; Huang, T. J. Thermal Behavior of Localized Surface Plasmon Resonance of Au/TiO_2 Core/Shell Nanoparticle Arrays. *Appl. Phys. Lett.* **2007**, *90*, 183117.
53. Li, D.; Paxton, W. F.; Baughman, R. H.; Huang, T. J.; Stoddart, J. F.; Weiss, P. S. Molecular, Supramolecular, and Macromolecular Motors and Artificial Muscles. *MRS Bull.* **2009**, *34*, 671–681.
54. Ye, T.; Kumar, A. S.; Saha, S.; Takami, T.; Huang, T. J.; Stoddart, J. F.; Weiss, P. S. Changing Stations in Single Bistable Rotaxane Molecules under Electrochemical Control. *ACS Nano* **2010**, *4*, 3697–3701.
55. Juluri, B. K.; Zheng, Y. B.; Ahmed, D.; Jensen, L.; Huang, T. J. Effects of Geometry and Composition on Charge-Induced Plasmonic Shifts in Gold Nanoparticles. *J. Phys. Chem. C* **2008**, *112*, 7309–7317.

56. Liu, Y. J.; Hao, Q.; Smalley, J. S. T.; Liou, J.; Khoo, I. C.; Huang, T. J. A Frequency-Addressed Plasmonic Switch Based on Dual-Frequency Liquid Crystals. *Appl. Phys. Lett.* **2010**, *97*, 091101.
57. Yang, S.; Guo, F.; Kiraly, B.; Mao, X.; Lu, M.; Huang, T. J. Microfluidic Synthesis of Multifunctional Janus Particles for Biomedical Applications. *Lab Chip* **2012**, *12*, 2097–2102.
58. Zheng, Y. B.; Kiraly, B.; Weiss, P. S.; Huang, T. J. Molecular Plasmonics for Biology and Nanomedicine. *Nanomedicine* **2012**, *7*, 751–770.
59. Madaria, A. R.; Kumar, A.; Ishikawa, F. N.; Zhou, C. Uniform, Highly Conductive, and Patterned Transparent Films of Percolating Silver Nanowire Network on Rigid and Flexible Substrates Using a Dry Transfer Technique. *Nano Res.* **2010**, *3*, 564–573.
60. Lee, C. H.; Kim, D. R.; Zheng, X. Fabricating Nanowire Devices on Diverse Substrates by Simple Transfer-Printing Methods. *Proc. Natl. Acad. Sci. U.S.A.* **2010**, *107*, 9950–9955.
61. Meitl, M. A.; Zhu, Z. -T.; Kumar, V.; Lee, K. J.; Feng, X.; Huang, Y. Y.; Adesida, I.; Nuzzo, R. G.; Rogers, J. A. Transfer Printing by Kinetic Control of Adhesion to An Elastomeric Stamp. *Nat. Mater.* **2006**, *5*, 33–38.
62. Sun, Y.; Rogers, J. A. Fabricating Semiconductor Nano/Microwires and Transfer Printing Ordered Arrays of Them onto Plastic Substrates. *Nano Lett.* **2004**, *4*, 1953–1959.
63. Takahashi, T.; Takei, K.; Adabi, E.; Fan, Z. Y.; Niknejad, A. M.; Javey, A. Parallel Array InAs Nanowire Transistors for Mechanically Bendable, Ultrahigh Frequency Electronics. *ACS Nano* **2010**, *4*, 5855–5860.
64. Chan, C. K.; Peng, H.; Liu, G.; Mcllwrath, K.; Zhang, X. F.; Huggins, R.; Cui, Y. High-Performance Lithium Battery Anodes Using Silicon Nanowires. *Nat. Nanotechnol.* **2008**, *3*, 31–35.